Original Article

ISSN Print 2231 – 3648
Online 2231 – 3656

DEVELOPMENT AND EVALUATION OF DRUG LOADED CONTROLLED RELEASE MUCOADHESIVE MICROCAPSULES USING VARIOUS POLYMERS AND TECHNIQUES IN MANAGEMENT OF TYPE-2 DIABETES

*[1]Santhosh Kumar Mankala, [2]Appanna Chowdary Korla, [3]Sammaiah Gade
*[1]Vaageswari College of Pharmacy, Ramakrishna Colony, Karimnagar, A.P, India-505 481.
[2]Roland Institute of Pharmaceutical Sciences, Berhampur, Orissa, India-760 010.
[3]University College of Pharmaceutical Sciences, Kakatiya University, Warangal, India-500 025.

Abstract

Type-2 diabetes is a metabolic disorder, resulting in hyperglycemia because the pancreatic β-cell does not produce enough insulin. Nateglinide is a meglitinide short-acting non-sulfonylurea, pancreatic, beta-cell-selective that improves overall glycemic control in type-2 diabetes, but nateglinide has short biological half-life of 1.5-2.5 h and therefore a controlled release medication is required to get prolonged effect with reduced fluctuations in drug plasma concentration levels. Microencapsulation and mucoadhesion techniques were found acceptable to achieve controlled release and drug targeting for many years. Mucoadhesion facilitates the intimate contact of the dosage form with the underlying absorption surface for improved bioavailability of drugs to prolong intestinal residence time. Nateglinide microcapsules were prepared by following orifice-ionic gelation technique (OIGT) and emulsion ionic gelation techniques (EIGT) employing SA (sodium alginate) as the coat material in combination with some mucoadhesive polymers such as (hydroxypropyl methylcellulose) HPMC, (sodium carboxy methylcellulose) Sod. CMC, carbopol and (methyl cellulose) MC (drug:SA:polymer at ratios 2:2:1, 2:3:1 and 2:4:1). Infrared spectroscopy, differential scanning calorimetry and X-ray diffraction studies proved the compositions were compatible without interaction between the drug and excepients. The prepared microcapsules were evaluated for various physical and release parameters. The resulted microcapsules were found to be discrete and spherical in scanning electron microscopy studies and free flowing in rheological studies. Particle size of microcapsules was found larger with OIGT around 756.54 ± 19.276 µm to 802.74 ± 29.325 µm and smaller with EIGT around 490.16 ± 12.124 µm to 531.61 ± 6.109 µm. The microencapsulation efficiency and swelling index was found to be higher in HPMC containing formulations with OIGT and in carbopol containing formulations with EIGT but, swelling index was found more in HPMC containing formulations. With both techniques microcapsules containing carbopol exhibited good mucoadhesive property in the *in vitro* wash-off test. *In vitro* drug release studies were carried out up to 24 h and they followed zero-order release kinetics with Case II and Super case II mechanisms. The drug release from the microcapsules was sustained over a prolonged period with greater retardation in drug:SA:HPMC (2:4:1) containing microcapsules prepared by OIGT technique, and this proved to be the best formulation.

Key words: Diabetes, Orifice ionic gelation, Emulsion ionic gelation, Mucoadhesive polymers.

Author for Correspondence:

Santhosh Kumar Mankala,
Vaageswari College of Pharmacy,
Karimnagar, A.P, India-505 481.
Email: inspiration.santosh@gmail.com

Introduction

Microcapsules can be defined as solid, approximately spherical particles made of polymeric, waxy or other protective materials ranging in size from 1 to 1000µm. Microencapsulation is a process used to achieve controlled release and drug targeting. Mucoadhesion

has been a topic of interest in the design of drug delivery systems to prolong the residence time of the dosage form in (gastrointestinal tract) GIT, which facilitates the intimate contact with the absorption surface to enhance the bioavailability of drugs. [1] Mucoadhesion is the process by which a natural or a synthetic polymer can be adhered to a (biological substrate) mucosal layer, and the phenomenon is known as mucoadhesion. The substrate possessing mucoadhesive property can help in devising a delivery system capable of delivering a drug for a prolonged period of time at a specific delivery site and offers several advantages over other oral controlled systems by virtue of prolongation of residence of the drug in GIT. Mucoadhesive microcapsules provide the needed continuous therapy in the management of type-2 diabetes with high margin of safety. [2, 3]

Several studies have reported on controlled drug delivery systems in the form of tablets, films, patches, and gels for oral, buccal, nasal, ocular, and topical routes. Nateglinide is made available as many forms in the market like conventional and simple sustained release tablets, but microencapsulation is a technique used to deliver the medicament at controlled rate by targeting. Microcapsules have more advantages over conventional and simple sustained release tablet formulations, such as targeting, less dosing frequency, zero-order release and high margin of safety, which are not possible with the existing formulations. Amongst the polymers used for microencapsulation, alginate has gained much attention since it is non toxic, biodegradable and can be prepared by a safe technique avoiding organic solvents. Hence orifice-ionic gelation technique and emulsion-ionic gelation technique was developed as an alternative approach even though so many other techniques are available like single and double emulsification techniques, normal and interfacial polymerization, coacervation phase separation, spray drying, spray congealing, etc. [4]

Diabetes is a clinically and genetically heterogeneous group of disorders/metabolic disorder affecting the metabolism of carbohydrates, lipids, and proteins. The characteristic feature of diabetes is an abnormal elevation in blood glucose levels (Hyperglycemia), is due to a deficiency of insulin secretion caused by pancreatic β-cell dysfunction and/or insulin resistance in liver and muscle. Diabetes is a syndrome in which chronic hyperglycemia leads to long-term damage to various organs including the heart, eyes, kidneys, nerves, and vascular system. This high blood sugar produces the classical symptoms of Polyuria (frequent urination), polydipsia (increased thirst) and polyphagia (increased hunger). This metabolic dysregulation is often associated with alterations in adipocyte metabolism. The current classification of diabetes is based upon the pathophysiology of each form of the disease. Type-1 diabetes results from cellular mediated autoimmune destruction of pancreatic b-cells, usually leading to total loss of insulin secretion. Type-1 diabetes is usually present in children and adolescents, although some studies demonstrated 15% to 30% of all cases being diagnosed after 30 years of age. The lack of insulin production in patients with type 1 diabetes makes the use of exogenous insulin necessary to sustain life, hence the former name "insulin-dependent diabetes." In the absence of insulin, these patients develop ketoacidosis, a life-threatening condition. Type-2 diabetes, previously called non–insulindependent diabetes, results from insulin resistance, which alters the use of endogenously produced insulin at the target cells. Type-2 patients have altered insulin production as well; however, autoimmune destruction of b-cells does not occur as it does in type-1, and patients retain the capacity for some insulin production. Because the type-2 patient still produces insulin, the incidence of ketoacidosis is very low compared to type-1 as insulin secretion becomes insufficient to compensate for insulin resistance. Although type-2 patients do not need insulin treatment to survive, insulin is often taken as part of the medical management of type-2 diabetes. [5]

Nateglinide is a metglinide short-acting, pancreatic, beta-cell-selective, KATP potassium channel blocker that improves overall glycemic control in type-2 diabetes. Although nateglinide's mechanism of action is related to that of sulphonyl-ureas, important differences do exist. Nateglinide binds rapidly to the sulfonylurea SUR_1 receptor with a relatively low affinity, and it dissociates from it extremely rapidly in a manner of seconds. This rapid association and dissociation gives nateglinide a unique "fast on-fast

off" effect. Thus, nateglinide has a rapid onset and short duration of action on beta cells in stimulating insulin secretion *in vivo* and providing good control of postprandial hyperglycemia when taken immediately prior to meals. This hypoglycemic effect of nateglinide leads to improved glycemic control, while the short duration avoids delayed hyperinsulinemia and hypoglycemia after meals. Nateglinide is not a sulfonylurea, but it shares the mechanism of action of commonly used oral hypoglycemic agents such as glibenclamide and glipizide. Like the recently introduced, short-acting agent, repaglinide, it does not incorporate a sulfonylurea moiety. Compounds with such a profile should not only achieve improved overall glucose control, but also reduce the risk of vascular complications which is the most important feature of nateglinide. Nateglinide is both effective and well tolerated in the treatment of type-2 diabetes. The reported overall profile of adverse effects appears to be superior to that of other KATP potassium channel blockers, the glucose modulator metformin and PPAR-gamma agonists such as troglitazone. Clinical comparisons of these agents have shown nateglinide to be more effective in attenuating postprandial glucose than any other oral hypoglycemic agent, and that treatment with nateglinide provides effects that afford improved control of plasma glucose levels. The administration regimen for nateglinide, immediately prior to meals, also facilitates patient compliance.[6] There are numerous drugs for treating type-2 diabetes, the objective of the present work was to develop, characterize (pre- and post-formulation parameters) nateglinide mucoadhesive microcapsules by following orifice-ionic gelation and emulsion-ionic gelation techniques using (Sod. Alginate) SA as the release rate retarding polymer, with (sodium carboxy methylcellulose) Sodium CMC, (hydroxypropyl methylcellulose) HPMC, Carbopol and (methylcellulose) MC as mucoadhesive polymers. And, to study the influence of techniques, mucoadhesive polymers and sodium alginate on physical and release properties of prepared microcapsules. Sod. CMC, HPMC, carbopol and MC are economic and easily available synthetic hydrophilic polymers and these can be extensively used for designing mucoadhesive delivery systems due to their ability to exhibit strong hydrogen bonding with the mucin present in the mucosal layer as compared to thiolated polymers, lectin-based polymers and other natural polymers. Basically, polymers of natural source containing polysaccharides, carbohydrates and cystine are be less stable as compared to those containing synthetic polymers as these are highly prone for microbial-degradation.[7]

Materials and Method

Nateglinide pure drug was obtained as a gift sample from M/s Hetero Drugs Ltd., Hyderabad, (Andhra Pradesh, India). HPMC, Sod. CMC, Carbopol and MC were procured from M/s Central Drug House (P) Ltd., (New Delhi, India). SA (having a viscosity of 5.5 cps in a 1% w/v aqueous solution at 25°C), calcium chloride and petroleum ether were procured from M/s S. D. Fine Chemicals Pvt. Ltd., Mumbai, (Maharastra, India).

Preparation of Nateglinide Mucoadhesive Microcapsules

Nateglinide mucoadhesive microcapsules were prepared by employing SA as the coat material in combination with four mucoadhesive polymers such as HPMC, Sod. CMC, Carbopol and MC (drug:SA:polymer at ratios 2:2:1, 2:3:1 and 2:4:1) by following orifice-ionic gelation technique (OIGT) and emulsion-ionic gelation technique (EIGT) [8-11]

Orifice-ionic gelation technique (OIGT): SA (2.0 g, 3.0 g and 4.0 g) and the mucoadhesive polymer (1.0 g) were dissolved in purified water (25 ml) to form a homogenous polymer solution to which core material; nateglinide (2.0 g) was added and mixed thoroughly to get smooth viscous dispersion. The resulting dispersion was then added drop wisely into 200 ml calcium chloride (10% w/v) solution through a syringe with a needle of No. 22 size. The added droplets were retained in the calcium chloride solution for 15 min to complete the curing reaction and to produce spherical rigid microcapsules. The microcapsules were separated by decantation and the product was washed with petroleum ether to remove water and dried at 45° C for 12 h. The prepared formulations were named as ONM_1 – ONM_{12} (Table 1). Emulsion-ionic gelation technique (EIGT): SA (2.0 g, 3.0 g and 4.0 g) and the mucoadhesive polymer (1.0 g) were dissolved in purified water (25 ml) to form a homogenous polymer solution to which core material;

nateglinide (2.0 g) was added and mixed thoroughly to get smooth viscous dispersion (Table 1). The viscous aqueous dispersion was then extruded through a syringe needle 23# into 200 ml of light liquid paraffin containing 1.5% span-80 and 0.2% glacial acetic acid being kept under magnetic stirring (Remi MS-301) at 500 rpm to undergo emulsification which then led to form spheres dispersed. 200 ml of (10% w/v) calcium chloride solution was poured with continuous stirring, by which the formed spheres were exposed towards the calcium chloride. The formed spheres were allowed to keep as such for 30 min to finish curing process. The microcapsules were then decanted and washed with petroleum ether to remove liquid paraffin and water and dried at 45° C for 12 h. The prepared formulations were named as ENM_1 – ENM_{12} (Table 1).

The stated ratios were fixed as per the results obtained in manual optimization of SA and mucoadhesive polymer. When drug:SA:polymer was less than 2:2:1, the formulation was found to disintegrate within a short time, and when the ratio was more than 2:4:1, the dosage form weight was increased to more than 1100 mg, making it difficult to fill in a capsule and the release was also retarded for more than 24 h. When the ratio of mucoadhesive polymer was decreased less than the fixed ratio formulations became non-adhesive, and when it was increased more than the fixed ratio, all the microcapsules became sticky and this also led to drying problem.

Evaluation of Prepared Microcapsules

Particle size analysis

All the batches prepared were analyzed for particle size where the microcapsules were placed on a set of standard sieves ranging from sieve No. 16# to 60#, using an electromagnetic sieve shaker (Electro Lab, EMS-8). The sieves were arranged in such a way that they were in a descending order with the mesh size 16# on the top and 60# mesh in the bottom. The microcapsules passed through the set of sieves and the amount retained on each sieve was weighed and the average mean diameter was determined and considered as mean particle size: [12]

$$\text{Mean Particle Size} = \frac{\sum(\text{Mean Particle Size of the Fraction X Weight Fraction})}{\sum(\text{Weight Fraction})} \quad \ldots. (1)$$

Bulk density

Accurately weighed microcapsules (M) were transferred into a 100 ml graduated cylinder to measure the apparent volumes or bulk volume (V_b). The measuring cylinder was tapped for a fixed period of time and tapped volume (V_t) occupied in the cylinder was measured. The bulk density and tapped/true density were calculated in gram per milliliter by the following formula: [13]

$$\text{Bulk Density}(\rho_b) = \frac{\text{Weight of Microcapsules (g)}(M)}{\text{Bulk Volume (ml)}(V_b)} \quad \ldots. (2)$$

$$\text{True/Tapped Density}(\rho_t) = \frac{\text{Weight of Microcapsules (g)}(M)}{\text{Tapped Volume (ml)}(V_t)} \quad \ldots. (3)$$

where, M = mass of the powder, V_b = bulk volume of the powder and V_t = tapped volume of the powder.

Carr's index and Hausner's ratio

The static angle of repose was measured according to the fixed funnel and free standing cone method. The bulk density of the mixed microcapsules was calculated for determining the Hausner's ratio and Carr's index from the poured and tapped bulk densities of a know weight of sample using a measuring cylinder. [14, 15] The following equations were used for the calculations:

$$\text{Carr's Index} = \left[\frac{\text{Tapped Density} - \text{Bulk Density}}{\text{Tapped Density}}\right] \times 100 \quad \ldots. (4)$$

$$\text{Hausner's Ratio} = \frac{\rho T}{\rho B} \quad \ldots. (5)$$

Angle of repose

A funnel was fixed in a stand in such a way that the top of the funnel was at a height of 6 cm from the surface. The microcapsules were passed from the funnel so that they formed a pile. The height and the radius of the heap were measured and the angle of repose was calculated using the equation. [13, 16]

$$\theta = \text{Tan}^{-1}\left[\frac{h}{r}\right] \ldots. (6)$$

Scanning Electron Microscopy (SEM)

The surface, morphology, microcapsules size, microcapsules shape, etc., were determined by using Scanning Electron Microscopy (BIOMETRICS: SEM-CS491Q/790Q). Dry microcapsules were placed on an electron microscope brass stub that was coated with gold (thickness 200 nm) in an ion sputter. Pictures of microcapsules were taken by random scanning of the stub under the reduced pressure (0.001 torr).

% Drug content evaluation

Nateglinide content in the microcapsules was estimated by UV-spectrophotometric method at a wavelength of 227 nm in phosphate buffer of pH 7.4, with 10% methanol (Elico, SL-158). The method obeyed Beer's law in the concentration range 10-50 µg/ml. Microcapsules containing equivalent to 100 mg of nateglinide were crushed as fine powder, extracted with 10 ml of methanol, and made up to 100 ml with pH 7.4 phosphate buffer. One milliliter of the sample solution was taken and made up to the volume to 10 ml with phosphate buffer pH 7.4, and the absorbance was measured at wavelength 227 nm. The procedure was repeated with pure nateglinide. The absorbance values from the pure drug nateglinide and microcapsules were treated and the %drug content was calculated. The method was validated for linearity, accuracy and precision.

Microencapsulation efficiency

Microencapsulation efficiency was calculated using the following formula: [17]

$$\text{Microencapsulation efficiency} = \left[\frac{\text{Estimated percentage drug content}}{\text{Theoratical percentage drug content}}\right] \times 100 \quad \ldots. (7)$$

Determination of wall thickness

Wall thickness of microcapsules was determined by using the equation: [18]

$$h = \frac{\Gamma(1-P)\,d_1}{3(Pd_2 + 1 - P)\,d_1} \quad \ldots. (8)$$

where, h = wall thickness, Γ = arithmetic mean radius of microcapsules, d_1 and d_2 are densities of core and coat material respectively, and P is the proportion of medicament in microcapsules. All the experimental units were studied in triplicate (n = 3).

Swelling index

Pre-weighed nateglinide microcapsules (W_0) formulated with mucoadhesive polymers by employing different coat: core ratios were placed in pH 7.4 phosphate buffer maintained at 37°C. After the 3rd hour, the microcapsules were collected and blotted to remove excess water and weighed (W_t). The swelling index was calculated with the following formulae: [19]

$$\text{Swelling Index} = \frac{W_t - W_0}{W_0} \times 100 \quad \ldots. (9)$$

where W_t = weight of microcapsules observed at the 3rd h and W_0 = the initial weight of microcapsules.

Permeability studies

The permeability constant P_m of the microcapsules was calculated using the equation: [20]

$$P_m = \frac{K \cdot V \cdot H}{A \cdot C_s} \quad \ldots. (10)$$

where V is the volume of the dissolution medium (cm^3), H the wall thickness of the microcapsules (mm), A the surface area of the microcapsules (cm^2), C_s the solubility of the core material (mg) in the dissolution medium and K is the release rate constant (mg/h^{-1} or h^{-1}).

For a given microcapsule and under standard testing conditions the values of V, A and C_s remain constant and hence the equation can be written as:

$$P_m = K \times H \quad \ldots. (11)$$

where K is the release rate constant and H is the wall thickness of the microcapsule.

Fourier Transform Infrared studies

Fourier Transform Infrared (FT-IR) analysis measurements of pure drug, carrier and drug-loaded microcapsules formulations were obtained using a Perkin-Elmer system 200FT-IR spectrophotometer. The pellets were prepared on KBr-press under a hydraulic pressure of 150 kg/cm^2; the spectra were scanned over the wave number range of 4000-400 cm^{-1} at the ambient temperature.

Differential scanning calorimetry (DSC)

Differential scanning calorimetry (DSC) was performed on nateglinide drug loaded microcapsules using Seiko (Japan) DSC model 220C. Samples were sealed in aluminum pans and the DSC thermograms were reported at a heating rate of 10°C/min from 20 to 260°C.

X-ray diffraction studies

Different samples were evaluated by X-ray powder diffraction. Diffraction patterns were obtained using X-ray diffractometer with a radius of 240 mm. The Cu Ka radiation was Ni filtered. A system of diverging and receiving slits of 1 and 0.1mm respectively was used. The pattern was collected with 40 kV of tube voltage and 30 mA of tube current and scanned over the 2Θ range of 10^0-80^0.

***In vitro* wash-off test for mucoadhesive microcapsules**

The mucoadhesive property of the microcapsules was evaluated by an *in vitro* adhesion testing method known as wash-off method. A piece of goat intestinal mucus (2 × 2 cm) was mounted onto glass slides of (3 × 1 inch) with elastic bands. Glass slide was connected with a suitable support. About 50 microcapsules were spread onto each wet tissue specimen, and thereafter the support was hung onto the arm of a USP tablet disintegrating test machine (Electro Lab, ED 2AL). The disintegration machine containing tissue specimen was adjusted for a slow, regular up and down moment in a test fluid at 37°C taken in a beaker. At the end of 1 h and later at hourly intervals up to 8 hours, the machine was stopped and the number of microcapsules still adhering onto the tissue was counted. The test was performed in phosphate buffer of pH 6.8. [21]

***In vitro* drug release studies of microcapsules**

In vitro drug release studies of microcapsules were carried out using USP XXIII Eight station dissolution rate test apparatus Type I with a basket stirrer (Electro Lab, EDT 08 LX) at 100 rpm in 900 ml 0.1 N HCl for the 1st 2 h, then in phosphate buffer of pH 7.4 at 50 rpm and temperature 37 ± 0.5°C. Microcapsules equivalent to 100 mg of nateglinide were tied in a muslin bag and kept in the basket. Five milliliter samples of the dissolution fluid were withdrawn at regular intervals and replaced with fresh quantity of dissolution fluid. The samples were filtered, diluted and analyzed, using Elico, SL-158 Double-beam UV-Visible Spectro - photometer at wavelength 221 and 227 nm respectively. For all the formulations, the dissolution was carried out in triplicates and statistically analyzed using InStat3®. The obtained data were used to calculate the % drug release and to determine the order and mechanism of the release. [22] The formulation showed that best release among prepared by both techniques was identified and prepared 6 times and 6 formulations form each batch were evaluated for drug release and the results were

statistically analyzed by analysis of variance (one factor ANOVA). [23]

Curve fitting analysis [24-27]

Zero-order release rate kinetics

To study the zero–order release kinetics, the release rate data are fitted to the following equation:

$$Q = K_0 t \quad \ldots. (12)$$

where "Q" is the fraction of drug released, "K" the release rate constant and "t" is the release time.

First-order kinetics

A first-order release would be predicated by the following equation:

$$\text{Log}C = \text{Log}C_o - \frac{Kt}{2.303} \quad \ldots. (13)$$

where; C = amount of drug remaining at time "t", Co = initial amount of the drug and K = first-order rate constant (h^{-1})

When the data are plotted as cumulative percent drug remaining versus time, it yields a straight line, indicating that the release follows first-order kinetics. The constant "K" can be obtained by multiplying 2.303 with slope.

Higuchi release model

To study the Higuchi release kinetics, the release rate data were fitted to the following equation:

$$Q = K.t^{1/2} \quad \ldots. (14)$$

where, "Q" is the amount of drug released, "K" the release rate constant, and "t" is the release time.

When the data are plotted as accumulative drug released versus square root of time, it yields a straight line, indicating that the drug was released by diffusion mechanism. The slope is equal to "K".

Korsmeyer-peppas release model

The release rate data were fitted into the following equation,

$$Mt/M\infty (Q) = K.t^n \quad \ldots. (15)$$

where, $Mt/M\infty$ is the fraction of drug released, "K" is the release constant, "t" is the release time, and "n" is the diffusion exponent for the drug released that is dependent on the shape of the matrix dosage form.

When the data are plotted as log of drug released versus log time, it yields a straight line with a slope equal to "n" and the "K" value can be obtained from Y intercept:

$$Q = Kt^n \ldots.. (16)$$

When n approximates 0.45, a Fickian/diffusion control release is implied: where $0.45 > n < 0.89$, it implies non-Fickian transport; and $n \geq 0.89$ for zero-order release.

Results and Discussion

The SEM and sieve analysis results showed the microcapsules to be discrete, spherical and free flowing. The particle size of microcapsules prepared by OIGT was found to be between 756.54 ± 19.276 µm and 802.74 ± 29.325 µm and of microcapsules prepared by EIGT was found to be between 490.16 ± 12.124 µm and 531.61 ± 6.109 µm (Figure 1). Angle of repose, bulk density, Carr's index and Hausner's ratio of microcapsules prepared by OIGT were found to be between 24.41 ± 0.52 and 27.74 ± 0.515, 0.499 ± 0.166 and 0.621 ± 0.104, 12.108 ± 4.576 and 23.824 ± 2.767 and 1.1377 ± 0.0455 and 1.3127 ± 0.0564, respectively where as in microcapsules prepared by EIGT was found to be between 23.2 ± 0.615 and 27.2 ± 0.522, 0.69 ± 0.034 and 0.83 ± 0.056, 12.643 ± 1.126 and 22.340 ± 1.341, and 1.144 ± 0.028 and 1.287 ± 0.018, respectively (Table 2a and 2b).

Drug excipient compatibility was proved by FT-IR spectroscopy, DSC and X-ray diffraction (XRD) studies. In the IR spectra of nateglinide, the pure drug formed a number of peaks prominently at different wave numbers, indicating the presence of functional groups like carboxyl, carbonyl and amino groups like peaks at 1701 cm^{-1} and 1724 cm^{-1} wave number were due to C-C and C=O stretching in aliphatic chain and ester. Prominent peaks at 1643 cm^{-1}, 1296 cm^{-1}, and 1446 cm^{-1} were appeared due to C=O stretching, C-O stretching and, C-O-H stretching in acidic group and peak at 1215 cm^{-1} wave number as stretching in aliphatic chain indicated the presence of carboxylic group and keto group in the structure. Broad peaks appeared between 2950 cm^{-1} and 2850 cm^{-1} wave number were due to C=C stretching in aromatic structure. Peaks appearing at 2931 cm^{-1} and 1408 cm^{-1} were because of C-H stretching aromatic and in CH_3 and CH_2 aliphatic respectively. A more intense peak was found between 3296 cm^{-1} and 3311 cm^{-1} because

of N-H stretching indicating the presence of amino group in the structure and peak at 1384 cm^{-1} wave number also indicates the presence of C-N stretching.

Peak at 1624 cm^{-1} was appeared because of –C-O-C stretching in SA. And all these peaks were appeared unchanged in IR spectra of combinations like nateglinide + SA + HPMC, nateglinide + SA + Sod.CMC, nateglinide + SA + Carbopol and nateglinide + SA + MC. The above interpretational data clearly states no interaction between the pure drug nateglinide and other excepients. Therefore, it can be said that the drug and excipients are compatible(Figure2).

The melting point of pure nateglinide was found to be 135.78 °C and followed endothermic type of reaction for which the onset was at 126.30°C and ended at 138.85 °C. The glass transition lag was found around 12.50°C and the same endothermic type of reactions was found in all combinations like nateglinide + SA + HPMC, nateglinide + SA + Sod.CMC, nateglinide + SA + Carbopol and nateglinide + SA + MC. No change was found in the melting point as well as glass transition lag, but special peaks were found indicating melting point of SA as 219.93°C, HPMC as 109.48°C, Sod. CMC as 109.71°C, Carbopol as 93.98°C and MC as 101.97°C, and the influence of excepients was found to be only in changing on's and end's sets of melting point peaks of nateglinide by absorbing heat but not by interactions.

The above interpretational data clearly indicate that the crystalline nature of the drug had not been changed and it did not undergo any polymorphism because there was no interaction, which has been proved by its unchanged melting point in all the combinational spectra. X-ray diffractogram of nateglinide proves its crystalline nature as evidenced from the number of sharp and intense peaks. The diffractogram of nateglinide with polymers showed diffused peaks indicating amorphous nature of the polymers and sharp, incense peaks indicating the crystalline nature of drug. Diffraction pattern of drug with polymer mixture showed simply the sum of the characteristic peaks of polymer indicating the presence of drug in crystalline form. Diffraction patterns of sample spectra represent the availability of crystalline peaks of drug situated at 12.83, 16.55, 20.01, 21.45, 25.76 and 38.21 (2θ) similar to the pure drug with corresponding intensities and linear counts respectively. The obtained 2θ values as characteristic peaks were found at the same position in combinations like nateglinide + SA + HPMC, nateglinide + SA + Sod. CMC, nateglinide + SA + Carbopol and nateglinide + SA + MC, but the intensities got reduced because of diffused peaks and more orientation in case of polymers. The reduction in intensities or linear counts of peaks in combinations was possibly due to decrease in the degree of crystallinity of the drug that might have occurred when the drug is well dispersed in the SA + polymer matrix. Finally the DSC and XRD data indicate that the crystallinity of pure drug was unchanged and stable, and indirectly show that the compositions are compatible. (Figures 3 and 4)

The microencapsulation efficiency in microcapsules by OIGT was from 80.892 ± 7.275 to 95.241 ± 2.341% with practical % drug content values around 22.65 ± 3.165 to 37.55 ± 1.113%, where as in microcapsules by EIGT microencapsulation efficiency was from 60.249 ± 1.997 to 95.638 ± 5.265% with practical % drug content values around 20.081 ± 0.49 to 33.483 ± 0.57% (Table 3a and 3b). Wall thickness and permeability coefficient were found around 88.51 ± 2.983 to 107.24 ± 4.328 μm and 454.011-590.62 $\mu g/cm^2/h$ respectively in microcapsules prepared with OIGT and in EIGT was found to be 57.988 ± 3.46 to 62.840 ± 3.24 μm and 332.627 to 352.079 $\mu g/cm^2/h$ respectively. In OGIT microcapsules swelling index was the highest in formulation ONM_3 around 221.23 ± 16.378% w/w and the least in ONM_{10} around 57.89 ± 12.554% w/w where as in EIGT microcapsules swelling index was found highest in formulation ENM_3 around 209.83 ± 12.338% w/w and the least in ENM_7 around 65.32 ± 18.123% w/w (Figure 5a and 5b). All microcapsules exhibited good mucoadhesive property in the *in vitro* wash-off test (Figure 6a and 6b) and microcapsules with carbopol ONM_9 and ENM_7 showed better mucoadhesion where 28% and 21% of microcapsules were found adhered to the mucosal layer after 8 h (Table 4a and 4b). In

formulations prepared by OIGT, the highest release 2.232% in formulation ONM_3 up to 24 h whereas the least retardation was observed to be around 98.216 ± 3.644% in the formulation ONM_4 after 16 h in *In vitro* drug release studies, but in formulations prepared by EIGT, the highest release retardation was found to be 99.345 ± 1.987% in formulation ENM_3 up to 20 h whereas the least retardation was found to be around 99.913 ± 3.857 % in formulation ENM_{10} up to 15 h (Figure 7a and 7b). When best retarding formulation was identified among microcapsules prepared by both techniques (ONM_3), the formulation was prepared 6 times (batches) and, six samples from each batch were taken then evaluated for drug release (n = 6) and statistically analyzed by (one factor ANOVA), the data showed Df_1 (5) and Df_2 (30) with an F-value of 2.0370. The obtained F-value found less than *f-table* value around 2.53 indicating less difference in between the groups and within the groups. *P-value* was found to be significant around 0.1017, proving maximum closeness between the results. All formulations followed zero-order non-Fickian release kinetics with Case II and Super Case II Transport mechanism (Table 5a and 5b).

All physical parameters were found in the acceptable range. The particle size and shape of microcapsules was influenced very much by the technique selected, microcapsules size was found smaller and more spherical with EIGT. The microencapsulation efficiency and mucoadhesive efficiency were found to be greater with Carbopol and HPMC than in other formulations and not much influence of mucoadhesive polymers were found on microencapsulation efficiency, whereas swelling index was higher in formulations with HCMC even prepared by both techniques. All compositions were found compatible in IR, DSC and XRD studies and thus are suitable for extending the scope of work in this research area. In mucoadhesion test it revealed that the formulations containing carbopol showed good mucoadhesion and its performance according to its percentage was found proportionate which was not found in other mucoadhesive polymers containing retardation was found to be around 99.637 ± formulations. The drug release from the microcapsules was sustained over an extended period of time. The study states that release not only depended on the core: coat ratio and type of mucoadhesive agent used, but also on the technique used in preparation where which got retarded as the coat material percentage got increased in both techniques.

Formulations prepared with OIGT showed more retardation as compared to EIGT. Microcapsules prepared using HPMC showed better sustained action, and formulation containing drug: SA: HPMC in the ratio 2:4:1 was found to be the best formulation as it released the maximum drug up to 24 h.

Conclusion

The mucoadhesive microencapsulation by following orifice-ionic gelation technique could be adopted in the laboratory as well as in the industry, as it is simple and reproducible. In conclusion, Carbopol and HPMC microcapsules could be used for better mucoadhesive action and SA could be used for better sustained action over an extended period of time. Release retardation depends not only on coat material percentage but also on mucoadhesive polymer selected and optimization of mucoadhesive polymer is needed to get formulations with desired quality. Selection of technique and optimization of technique found important to get desirable physical and release properties. Formulations prepared with OIGT produced more efficient microcapsules as compared to EIGT. However, further *in vivo* studies are needed to optimize the drug for sustained action in human beings for better bioavailability, and efficacy, and thus safety.

Acknowledgement

Authors wish to thank M/s Aurobindo Pharmaceuticals Ltd., Hyderabad, (Andhra Pradesh, India) for providing gift sample of Nateglinide, and authors will be thankful to management of Vaageswari College of Pharmacy, Karimnagar, (Andhra Pradesh, India) for supporting us to finish up this study successfully.

Table 01: Composition of various batches of nateglinide mucoadhesive microcapsules

S. No	Ingredients	Qty used in formulations (g)											
		ONM_1 ENM_1	ONM_2 ENM_2	ONM_3 ENM_3	ONM_4 ENM_4	ONM_5 ENM_5	ONM_6 ENM_6	ONM_7 ENM_7	ONM_8 ENM_8	ONM_9 ENM_9	ONM_{10} ENM_{10}	ONM_{11} ENM_{11}	ONM_{12} ENM_{12}
1.	Nateglinide	2	2	2	2	2	2	2	2	2	2	2	2
2.	Sod.Alginate	2	3	4	2	3	4	2	3	4	2	3	4
3.	HPMC	1	1	1	-	-	-	-	-	-	-	-	-
4.	SCMC	-	-	-	1	1	1	-	-	-	-	-	-
5.	Carbopol	-	-	-	-	-	-	1	1	1	-	-	-
6.	MC	-	-	-	-	-	-	-	-	-	1	1	1
Total Weight		5	6	7	5	6	7	5	6	7	5	6	7
Drug:SA:Polymer		2:2:1	2:3:1	2:4:1	2:2:1	2:3:1	2:4:1	2:2:1	2:3:1	2:4:1	2:2:1	2:3:1	2:4:1

Table 02a: Physical parameters data of nateglinide mucoadhesive microcapsules ONM_1-ONM_{12}

Formulation	Angle of Repose	Bulk Density (g/cm3)	Carr's Index	Hausner's Ratio	Mean Particle Size (µm)	Wall Thickness (µm)	Permeability coefficient (µg/cm²/hr)
ONM_1	25.96 ±1.827	0.54 ±0.0875	15.76 ±1.557	1.1870 ±0.0979	765.92 ±19.856	89.610 ±6.345	541.208
ONM_2	27.11 ±0.52	0.529 ±0.0536	23.824 ±2.767	1.3127 ±0.0564	782.65 ±15.678	98.881 ±3.244	481.293
ONM_3	25.96 ±0.749	0.573 ±0.083	18.634 ±3.785	1.2290 ±0.0647	802.74 ±29.325	107.24 ±4.328	454.011
ONM_4	27.74 ±0.515	0.58 ±0.103	19.96 ±3.578	1.2493 ±0.0436	756.54 ±19.276	88.51 ±2.983	577.164
ONM_5	24.93 ±0.52	0.512 ±0.0757	17.056 ±4.536	1.2056 ±0.0787	782.34 ±23.234	98.843 ±3.762	554.815
ONM_6	24.41 ±1.202	0.542 ±0.0452	14.364 ±2.869	1.1677 ±0.0546	797.12 ±14.761	106.492 ±3.543	520.106
ONM_7	25.96 ±1.241	0.566 ±0.0127	13.968 ±3.896	1.1623 ±0.0768	762.34 ±23.432	89.189 ±2.675	542.563
ONM_8	25.56 ±1.294	0.602 ±0.0936	12.108 ±4.576	1.1377 ±0.0455	775.6 ±41.29	97.997 ±7.435	531.986
ONM_9	25.45 ±1.25	0.621 ±0.104	15.544 ±5.31	1.1840 ±0.0756	793.2 ±36.23	105.971 ±6.648	558.922
ONM_{10}	24.93 ±0.302	0.498 ±0.166	14.344 ±4.675	1.1674 ±0.0435	758.9 ±18.127	88.791 ±2.961	590.62
ONM_{11}	24.41 ±0.749	0.532 ±0.0972	15.944 ±1.979	1.1896 ±0.0768	770.6 ±33.849	97.365 ±4.552	587.062
ONM_{12}	27.11 ±0.202	0.565 ±0.0632	12.99 ±4.765	1.1492 ±0.0787	785.4 ±29.556	104.929 ±5.873	579.963

*Mean ± S.D (n=3)

Table 02b: Physical parameters data of nateglinide mucoadhesive microcapsules ENM_1-ENM_{12}

Formulation	Angle of Repose	Bulk Density (g/cm3)	Carr's Index	Hausner's Ratio	Mean Particle Size (μm)	Wall Thickness (μm)	Permeability coefficient (μg/cm²/hr)
ENM_1	25.4 ±0.617	0.76 ±0.035	15.555 ±1.052	1.184 ±0.023	490.16 ±12.124	57.988 ±3.46	352.079
ENM_2	26.3 ±0.721	0.79 ±0.046	17.708 ±1.141	1.215 ±0.026	510.46 ±5.324	60.355 ±2.65	341.573
ENM_3	27.2 ±0.522	0.72 ±0.057	21.739 ±.0943	1.277 ±0.0199	530.22 ±8.46	62.721 ±2.77	337.596
ENM_4	25.3 ±0.731	0.73 ±0.062	22.340 ±1.341	1.287 ±0.018	528.97 ±5.39	62.485 ±4.23	335.007
ENM_5	24.6 ±0.916	0.69 ±0.034	15.853 ±1.128	1.188 ±0.022	510.43 ±10.83	60.355 ±5.43	341.516
ENM_6	25.2 ±0.632	0.78 ±0.042	14.285 ±1.092	1.166 ±0.031	525.22 ±5.328	62.130 ±5.44	332.627
ENM_7	24.8 ±0.742	0.81 ±0.094	12.903 ±1.324	1.148 ±0.021	528.19 ±8.197	62.485 ±3.65	335.803
ENM_8	24.3 ±0.912	0.80 ±0.072	13.978 ±1.111	1.162 ±0.027	531.61 ±6.109	62.840 ±3.24	336.395
ENM_9	25.7 ±.0.844	0.79 ±0.046	13.186 ±1.223	1.151 ±0.027	500.84 ±13.203	59.171 ±3.44	348.085
ENM_{10}	23.2 ±0.615	0.76 ±0.065	12.643 ±1.126	1.144 ±0.028	498.37 ±12.983	58.934 ±4.25	349.183
ENM_{11}	25.6 ±0.712	0.81 ±0.046	13.829 ±1.091	1.160 ±0.019	506.26 ±10.462	59.881 ±3.87	348.591
ENM_{12}	24.8 ±0.827	0.83 ±0.056	13.541 ±1.232	1.156 ±0.026	512.69 ±8.236	60.591 ±2.44	340..360

*Mean ± S.D (n=3)

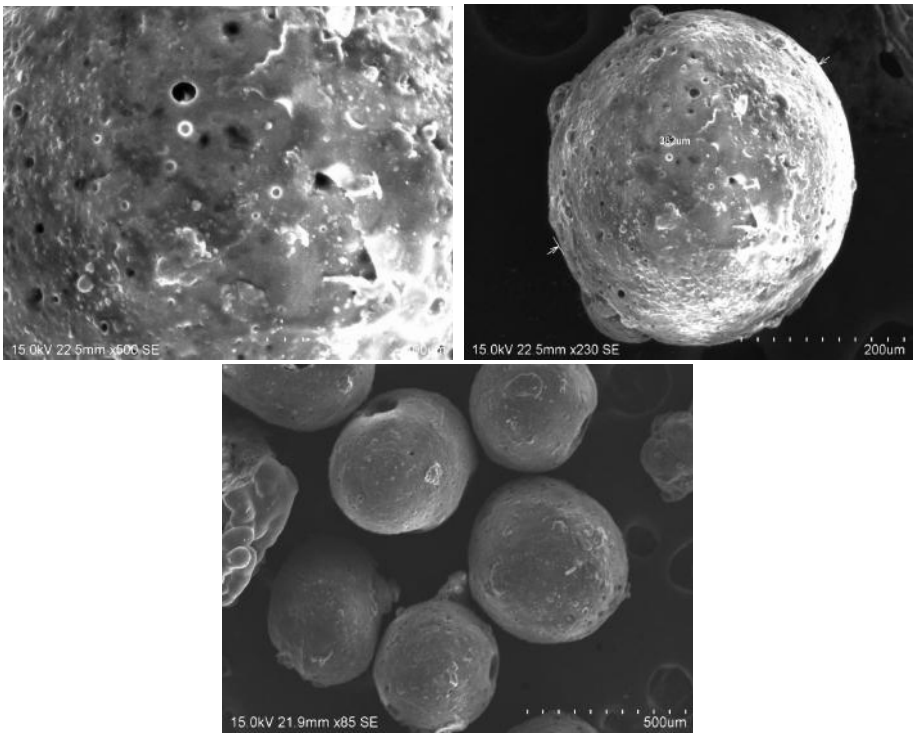

Figure 01: SEM pictograms of nateglinide mucoadhesive microcapsules prepared with EIGT

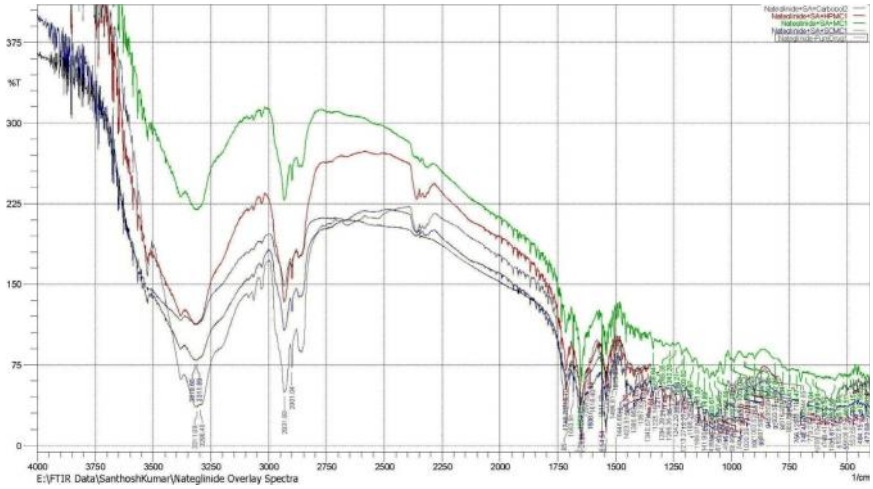

Figure 02: FT-IR spectra of nateglinide pure drug, nateglinide+SA+HPMC, nateglinide+SA+Sod.CMC, nateglinide+SA+Carbopol and nateglinide+SA+MC.

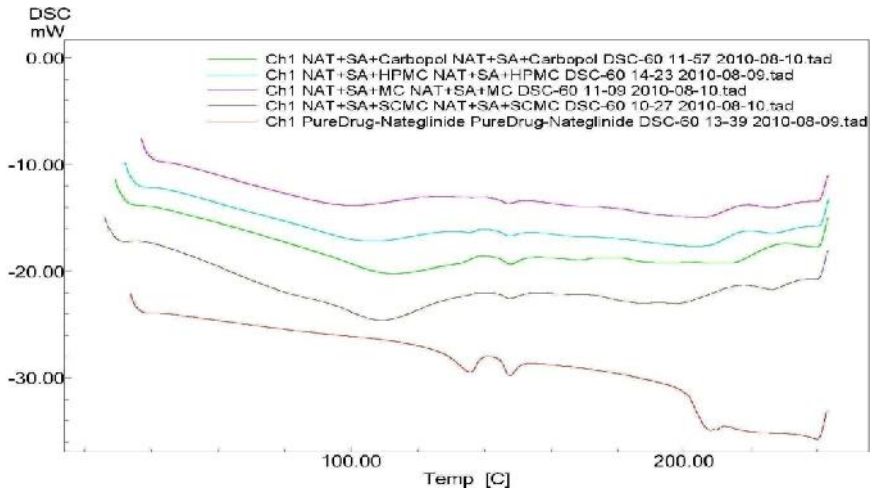

Figure 03: DSC spectra of nateglinide pure drug, nateglinide+SA+HPMC, nateglinide+SA+Sod.CMC, nateglinide+SA+Carbopol and nateglinide+SA+MC.

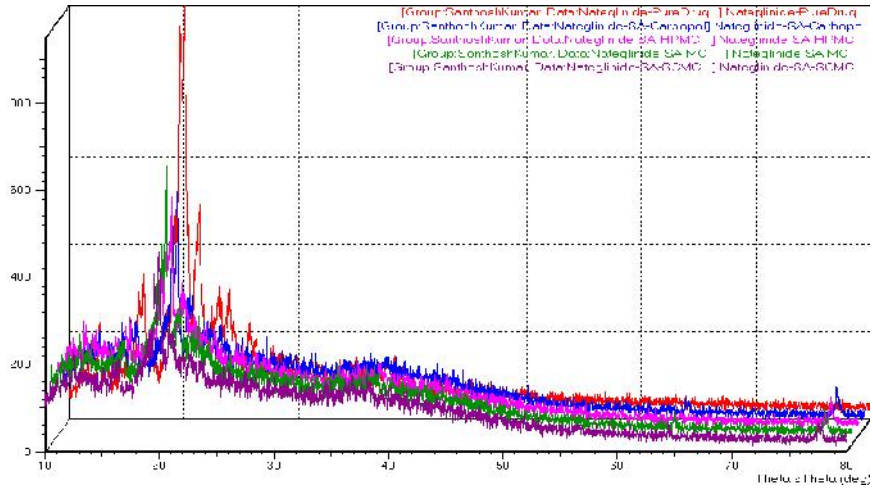

Figure 04: X-Ray diffraction spectra of nateglinide pure drug, nateglinide+SA+HPMC,

nateglinide+SA+Sod.CMC, nateglinide+SA+Carbopol and nateglinide+SA+MC.

Table 03a: Drug content/Encapsulation Efficiency of formulations ONM_1-ONM_{12}

Formulation	D:SA:P ratio	Weight Taken (mg)	Theoretical Drug Content (mg)	Practical Drug Content (mg)	Encapsulation Efficiency (%)
ONM_1	2:2:1	100	40	37.55 ±1.113	93.875 ±2.563
ONM_2	2:3:1	100	33.33	31.43 ±0.912	95.241 ±2.341
ONM_3	2:4:1	100	28.57	22.66 ±2.284	80.922 ±5.323
ONM_4	2:2:1	100	40	36.55 ±2.254	91.375 ±5.126
ONM_5	2:3:1	100	33.33	30.98 ±1.975	93.878 ±4.356
ONM_6	2:4:1	100	28.57	25.36 ±1.991	90.571 ±4.198
ONM_7	2:2:1	100	40	36.52 ±2.131	91.31 ±5.119
ONM_8	2:3:1	100	33.33	30.12 ±1.018	91.272 ±2.641
ONM_9	2:4:1	100	28.57	24.32 ±1.736	86.857 ±3.971
ONM_{10}	2:2:1	100	40	34.58 ±2.321	86.45 ±6.124
ONM_{11}	2:3:1	100	33.33	30.24 ±1.012	91.636 ±2.448
ONM_{12}	2:4:1	100	28.57	22.65 ±3.165	80.892 ±7.275

*Mean ± S.D (n=3)

Table 03b: Drug content/Encapsulation Efficiency of formulations ENM_1-ENM_{12}

Formulation	D:SA:P ratio	Weight Taken (mg)	Theoretical Drug content (mg)	Practical Drug Content (mg)	Encapsulation Efficiency (%)
ENM_1	2:2:1	100	40	32.151 ±0.543	80.377 ±2.343
ENM_2	2:3:1	100	33.33	28.833 ±0.488	86.507 ±1.998
ENM_3	2:4:1	100	28.57	25.136 ±0.682	87.980 ±3.146
ENM_4	2:2:1	100	40	33.213 ±0.467	83.032 ±1.987
ENM_5	2:3:1	100	33.33	30.092 ±0.656	90.285 ±2.345
ENM_6	2:4:1	100	28.57	24.047 ±0.491	84.168 ±2.675
ENM_7	2:2:1	100	40	32.372 ±0.585	80.93 ±3.782
ENM_8	2:3:1	100	33.33	20.964 ±0.682	62.898 ±4.353
ENM_9	2:4:1	100	28.57	27.324 ±0.766	95.638 ±5.265
ENM_{10}	2:2:1	100	40	33.483 ±0.57	83.707 ±3.265
ENM_{11}	2:3:1	100	33.33	20.081 ±0.49	60.249 ±1.997
ENM_{12}	2:4:1	100	28.57	21.503 ±0.551	75.264 ±2.897

*Mean ± S.D (n=3)

Table 04a: *In Vitro* Wash off Test Data of formulations ONM_1-ONM_{12}

Formulation (50 microcapsules)	% of microcapsules (±SD) adhering to tissue at (h)			
	Phosphate buffer, pH 7.4			
	1	2	4	8
ONM_1	54 ±7.33	42 ±5.66	32 ±4.33	16 ±2.66
ONM_2	66 ±4.33	52 ±3.33	32 ±3.66	24 ±3
ONM_3	76 ±6	62 ±5.33	48 ±4	22 ±3.33
ONM_4	52 ±4.66	44 ±2.66	34 ±2	18 ±3.33
ONM_5	68 ±5.33	56 ±4	44 ±3.33	22 ±2.66
ONM_6	82 ±5	68 ±4.33	58 ±4.66	20 ±1.66
ONM_7	64 ±4.66	52 ±3.66	38 ±2.33	16 ±3
ONM_8	76 ±3.66	56 ±4.33	44 ±3.33	26 ±2.33
ONM_9	92 ±6	66 ±5.66	52 ±3.66	28 ±3.33
ONM_{10}	52 ±3.33	44 ±4.33	34 ±2.66	18 ±3
ONM_{11}	62 ±2.66	56 ±2.66	43 ±3.33	24 ±3.66
ONM_{12}	76 ±4.66	62 ±4	48 ±2.66	20 ±2.66

*Mean ± S.D (n=3)

Table 04b: *In Vitro* Wash off Test Data of formulations ENM_1-ENM_{12}

Formulation (50 microcapsules)	% of microcapsules (±SD) adhering to tissue at (h)			
	Phosphate buffer, pH 7.4			
	1	2	4	8
ENM_1	74 ±3.66	51 ±4.66	33 ±5	12 ±4.33
ENM_2	48 ±2.33	36 ±5	21 ±6.66	15 ±2.66
ENM_3	52 ±5.66	39 ±7.66	23 ±5.33	08 ±4.33
ENM_4	78 ±3.33	59 ±8.33	22 ±4.33	7 ±3.66
ENM_5	65 ±5.66	42 ±6.33	29 ±6.33	10 ±3.33
ENM_6	62 ±6	40 ±5.66	24 ±5.66	11 ±4.66
ENM_7	49 ±7.33	41 ±7.33	36 ±4.66	21 ±3.33
ENM_8	80 ±2.33	57 ±4.66	40 ±7.33	13 ±5.33
ENM_9	72 ±5.66	56 ±5.33	41 ±6.66	18 ±4.33
ENM_{10}	58 ±7.66	43 ±7.33	27 ±5.33	11 ±3.33
ENM_{11}	56 ±6.33	44 ±4.33	25 ±6.33	9 ±4.33
ENM_{12}	67 ±6	42 ±5.66	23 ±4.33	11 ±3.66

*Mean ± S.D (n=3)

Table 05a: Release Kinetic Data of Formulations ONM_1-ONM_{12}

Formulation	Zero Order	Release rate constant	First Order	Higuchi	Best Fit	Korsmeyer-Peppas		Release Mechanism
	r^2	K_0	r^2	r^2		r^2	n	
ONM_1	0.9892	6.0396	0.8757	0.9433	Zero order	0.9864	1.2044	Super Case II
ONM_2	0.9831	4.8674	0.8577	0.9589	Zero order	0.9751	1.1132	Super Case II
ONM_3	0.9929	4.2336	0.7406	0.9644	Zero order	0.976	0.9716	Super Case II
ONM_4	0.9952	6.5209	0.8519	0.9462	Zero order	0.9859	1.086	Super Case II
ONM_5	0.9981	5.6131	0.7844	0.9297	Zero order	0.9871	0.9335	Super Case II
ONM_6	0.9759	4.884	0.8918	0.9611	Zero order	0.9778	1.1674	Super Case II
ONM_7	0.996	6.0833	0.7803	0.9466	Zero order	0.9878	0.9682	Super Case II
ONM_8	0.9965	5.4286	0.779	0.9391	Zero order	0.9809	1.2614	Super Case II
ONM_9	0.9868	5.2743	0.8665	0.9589	Zero order	0.9834	1.2527	Super Case II
ONM_{10}	0.9933	6.6518	0.6893	0.9019	Zero order	0.9941	1.2334	Super Case II
ONM_{11}	0.9828	6.0295	0.9146	0.9483	Zero order	0.9827	1.1442	Super Case II
ONM_{12}	0.991	5.5272	0.8374	0.9587	Zero order	0.9916	0.9973	Super Case II

Table 05b: Release Kinetic Data of Formulations ENM_1-ENM_{12}

Formulation	Zero Order	Release rate constant	First Order	Higuchi	Best Fit	Korsmeyer-Peppas		Release Mechanism
	r^2	K_0	r^2	r^2		r^2	n	
ENM_1	0.9873	6.9612	0.8140	0.9282	Zero order	0.9884	1.2174	Super Case II
ENM_2	0.9893	6.3850	08387	0.9359	Zero order	0.9929	1.2191	Super Case II
ENM_3	0.9965	5.1268	0.7567	0.9526	Zero order	0.9921	0.9586	Super Case II
ENM_4	0.9886	7.042	0.7864	0.9457	Zero order	0.9773	1.0587	Super Case II
ENM_5	0.9867	5.718	0.6094	0.8992	Zero order	0.9865	0.9312	Super Case II
ENM_6	0.9789	5.8049	0.8366	0.9572	Zero order	0.9882	1.0520	Super Case II
ENM_7	0.9891	6.3172	0.7834	0.9458	Zero order	0.9825	0.9414	Super Case II
ENM_8	0.9957	5.7242	0.6517	0.9545	Zero order	0.9987	0.9915	Super Case II
ENM_9	0.9833	5.697	0.8152	0.9613	Zero order	0.9852	1.0122	Super Case II
ENM_{10}	0.9937	7.0279	0.6713	0.9250	Zero order	0.9806	1.0253	Super Case II
ENM_{11}	0.9922	6.9825	0.8069	0.9424	Zero order	0.9863	1.0221	Super Case II
ENM_{12}	0.9968	5.9401	0.6868	0.9494	Zero order	0.9930	1.0396	Super Case II

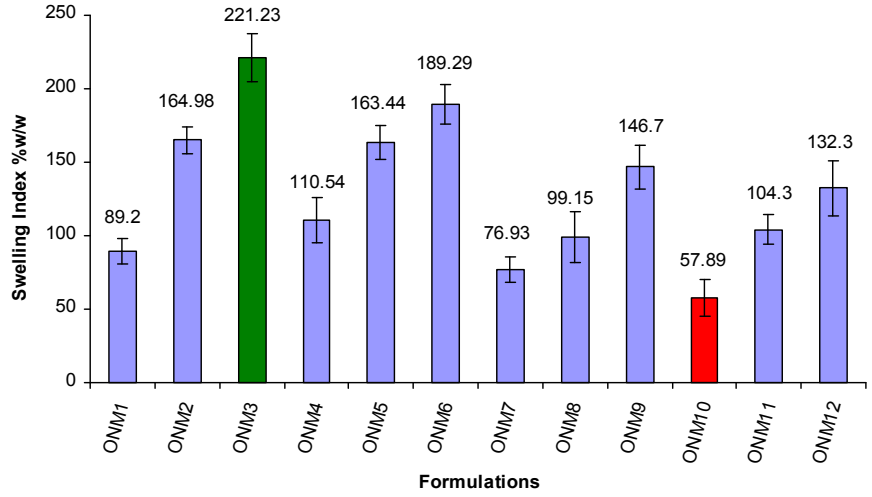

Figure 05a: Swelling Index histogram of nateglinide mucoadhesive microcapsules ONM_1-ONM_{12}

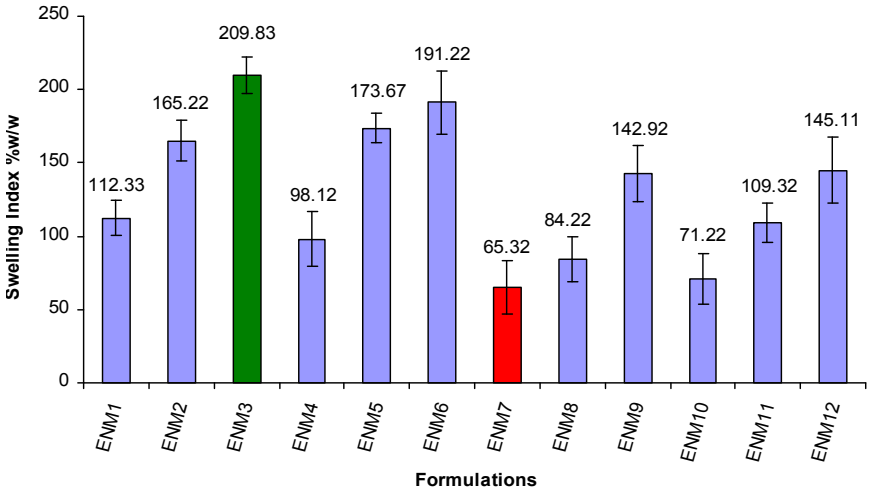

Figure 05b: Swelling Index histogram of nateglinide mucoadhesive microcapsules ENM_1-ENM_{12}

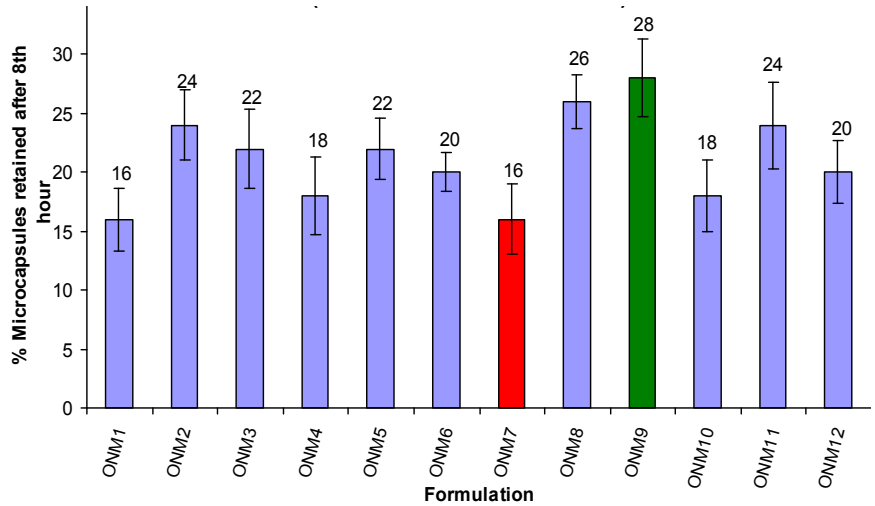

Figure 06a: *In vitro* mucoadhesive wash off test results histogram of nateglinide mucoadhesive microcapsules ONM_1-ONM_{12} after 8th hour

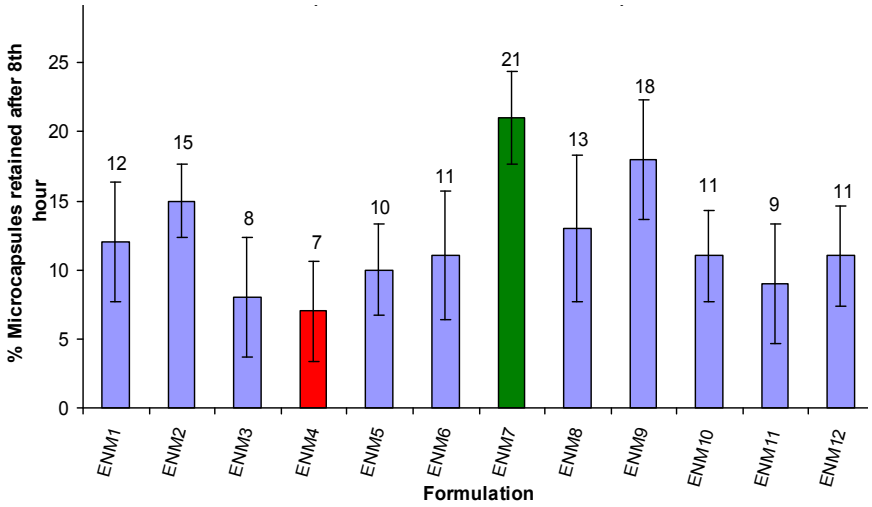

Figure 06b: *In vitro* mucoadhesive wash off test results histogram of nateglinide mucoadhesive microcapsules ENM$_1$-ENM$_{12}$ after 8th hour

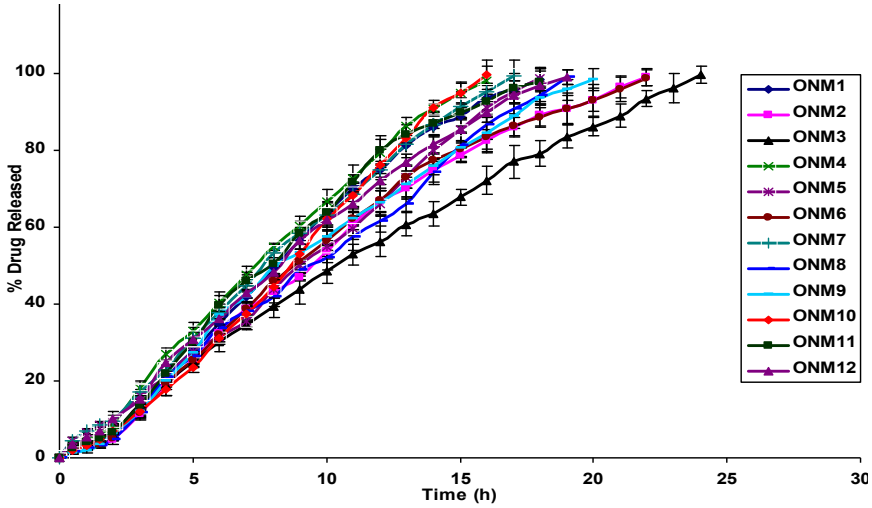

Figure 07a: *In vitro* drug release plots of nateglinide mucoadhesive microcapsules ONM$_1$-ONM$_{12}$

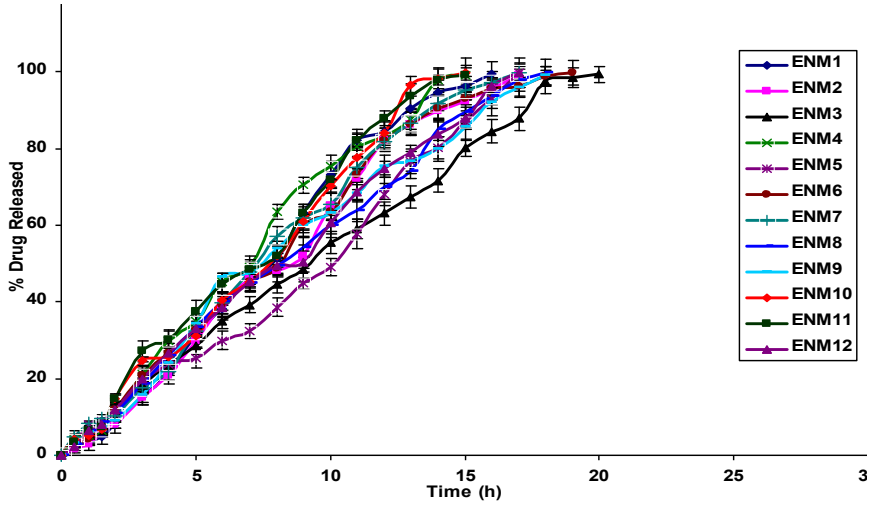

Figure 07b: *In vitro* drug release plots of nateglinide mucoadhesive microcapsules ENM$_1$-ENM$_{12}$

References

1. Robinson RJ, Lee VH. Controlled Drug Delivery: Fundamentals and Applications. Revised and expanded. Vol 29; 2nd ed. New York: Marcel Dekker Inc; 2005. pp. 9-19.
2. Boddupalli BM, Mohammed ZNK, Ravinder Nath A, Banji D. Mucoadhesive drug delivery system: An overview. *J Adv Pharm Tech Res*. 1, 2010, 381-387.
3. Pranshu TSK, Sathish MNV. Mucoadhesive drug delivery: mechanism and methods of evaluation. *Int J Pharma Bio Sci*. 2(1), 2011, 458-467.
4. Solmaz D, Reza A, Mohammadreza A and Ramin K. Formulation Optimization of Nifedipine Containing Microspheres Using Factorial Design. *African J Pharm Pharmacology*. 4(6), 2010, 346-354.
5. Mealey BL, Oates TW. Diabetes Mellitus and periodontal diseases. *J Periodontal*. *77*(8), 2006, 1289-1303.
6. Norman P, Rabasseda X. Nateglinide: A structurally novel, short-acting, hypoglycemic agent. *Drugs Today*. 37(6), 2001, 411-426.
7. Carvalho *FC*, Bruschi *ML*, Evangelista RC, Gremião MPD. Mucoadhesive drug delivery systems. *Brazilian J Pharm Sci*. 46(1), 2010, 1-17.
8. Chowdary KPR, Srinivas L. Mucoadhesive drug delivery system: Status of Current review. *Indian Drugs*. 37, 2000, 400-410.
9. Liu XD, Yu WY, Zhang Y, Xue WM, Yu WT, Xiong Y, *et al*. Characterization of structure and diffusion behavior of Ca–alginate beads prepared with external or internal calcium sources. *J Microencapsulation*. 18, 2002, 775-782.
10. Bahadur S, Chanda R, and Roy A, Preparation and evaluation of mucoadhesive microcapsules of captopril for oral controlled release. *Res J Pharm Tech*. 1(2), 2008, 100-105.
11. Kosaraju K, Ramakrishna R, Suarcharla RL, Murthy TEGK. Design and development of alginate beads containing mucoadhesive polymers of an oral controlled release of glimepiride. *Tech Spectrum*. 1(3), 2007, 22-28.
12. Lachman L, Lieberman HA, Kanig JL. The theory and practice of industrial pharmacy. 3rd ed. Bombay: Varghese Publishing House; 1987. pp. 22-28.
13. Puttewar TY, Kshirsagar MD, Chadewar AV, Chikale RV. Formulation and evaluation of orodispersible tablet of taste masked doxylamine succinate using ion exchange resin. *J King Saud Uni*. 22, 2010, 229-240.
14. Hausner HH. Friction conditions in a mass of metal powder. *Int J Metall*. 3, 1967, 7-13.
15. Carr RL. Evaluating flow properties of solids. *Chem Eng*. 72, 1965, 163-168.
16. Aulton ME. Pharmaceutics: The Science of Dosage Form Design. 3rd ed. New York: Churchill Livingstone; 1988: pp. 605-613.
17. Zinutti C, Hoffman M. Preparation and characterization of ethyl cellulose microspheres containing 5-fluoro-uracil. *J Microencapsul*. 11(5), 1994,555-563.
18. Si-Nang L, Carlier PF, Delort P, Gazzola J, Labont D. Determination of coating thickness of microcapsules and influence upon diffusion. *J Pharm Sci*. 62(3), 1973, 452-455.
19. Ma XJ, Xie YB, Zhou L, Yu XJ, Yuan Q, Li CC, *et al*. Relationship between preparation conditions and membrane strength of APA biomicrocapsules. *Chinese J Organ Transplantation*. 16, 1995, 156-157.
20. Koida Y, Kobayashi M, Samejima M. Studies on microcapsules. IV: Influence of properties of drugs on microencapsulation and dissolution behavior. *Chem Pharma Bull*. 34(8), 1986, 3354-3361.
21. Lehr CM, Bowstra JA, Tukker JJ, Junginer HE. Intestinal transit of bioadhesive microspheres in an *in situ* loop in the rat. *J Control Rel*. 13(1), 1990, 51-62.
22. Costa P, Jose-Manuel SL. Modeling and comparison of dissolution profiles. *Eur J Pharma Sci*. 13, 2001, 123-133.
23. Yadav A, Jain DK. Gastroretentive microbaloons of metformin: Formulations development and characterization. *J Adv Pharm Tech Res*. 2, 2011, 51-55.
24. The Indian Pharmacopoeia, Vol-II, Indian Pharmacopoeia Commission, Ghaziabad, 2007. pp. 740-742.
25. Higuchi T. Mechanism of Sustained Action Medication: Theoretical Analysis of Rate of Release of Solid Drug Dispersed in Solid Matrices. *J Pharm Sci*. 52, 1963, 1145-1149.
26. Ritger PL, Peppas NA. The simplest equation for description of solute release II. Fickian and anomalous release from swellable devices. *J Controlled Rel*. 52, 1987, 37-42.
27. Sipemann J, Peppas NA, Modeling of drug release for delivery systems based on hydroxypropyl methyl cellulose (HPMC). *Adv Drug Del Rev*. 2(48), 2001, 139-157.